The background of the slide is a dark blue-grey color. It features a faint, light-grey map of Japan. Overlaid on the map is a compass rose with a needle pointing towards the top-left. The needle has a small 'N' at its tip. The compass rose also includes degree markings and some other symbols like a dollar sign and a triangle.

Recent progresses on Active Fault Researches in Japan

- Contribution of Geological Survey of Japan

Eikichi Tsukuda, Yuuichi Sugiyama
Active Fault Research Center,
Geological Survey of Japan, AIST

Contents

Researches of Active Fault Research Center

Researches for Major Active Faults

Hazard Assessment of Osaka basin

International Cooperation US-Japan

**Active Fault Research Center
(AFRC)
SINCE APRIL 2001**

**Geological Survey of Japan
(New GSJ)
National Institute
of Advanced Industrial Science
and Technology (new AIST)**

Active Fault Research Center (AFRC) since 2001

Active Fault Research Center (AFRC) is launched in April 2001 as one of major research units of the new Geological Survey of Japan (GSJ), according to the establishment of National Institute of Advanced Industrial Science and Technology (AIST). AFRC is one of responsible organizations for active faults studies in Japan under the Headquarters for Earthquake Research Promotion of the Japanese government (HQERP). AFRC will make possible efforts to provide innovative, reliable scientific results to help reduce losses from future earthquakes and tsunamis.

Mission of AFRC

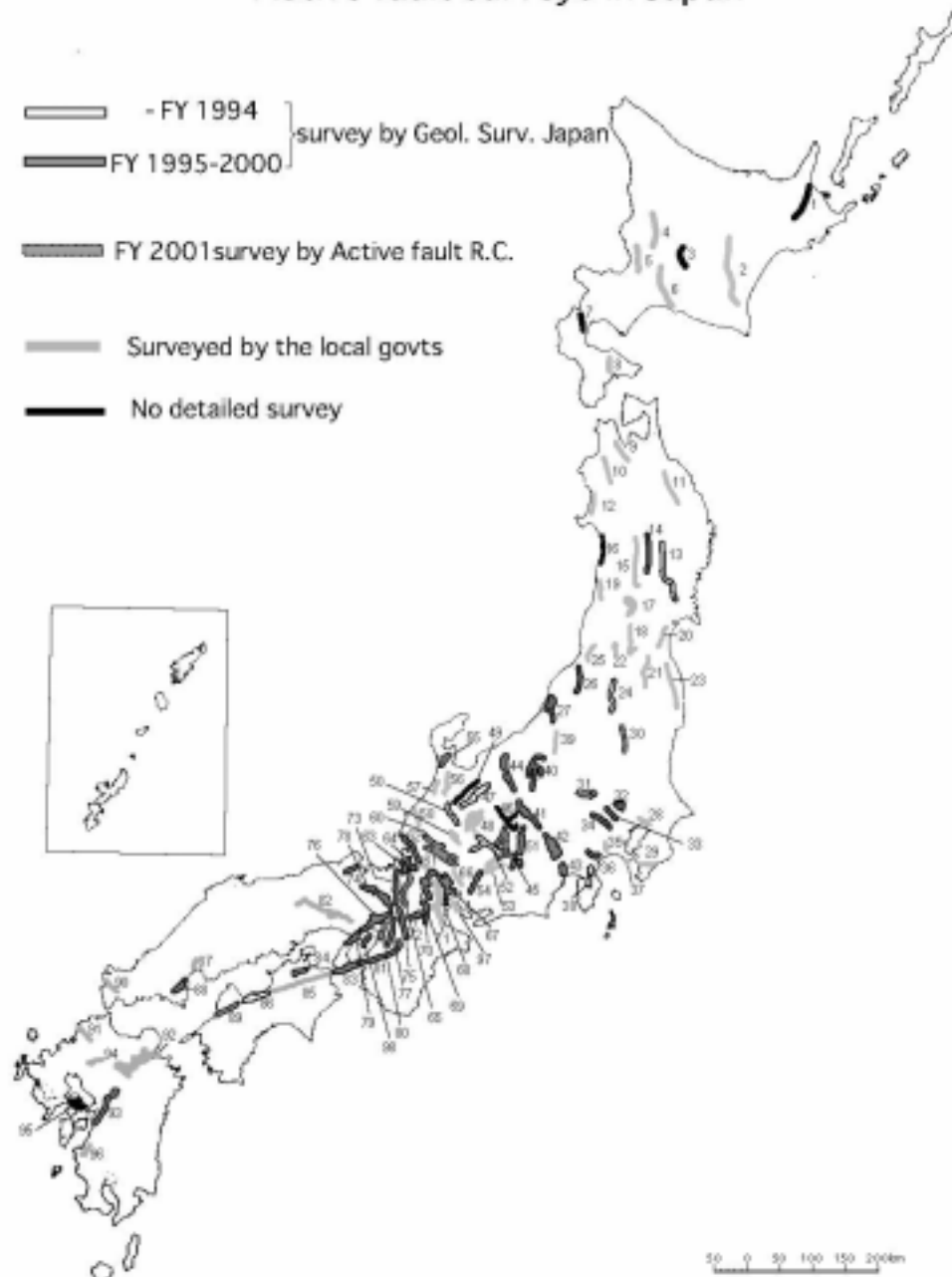
Active fault survey and evaluation for future activity

Assessing earthquake hazards by fault geometry, subsurface geology, fault modeling, strong motion evaluation

Public outreach

Survey result papers, Maps, Database

Active fault surveys in Japan



Active fault survey in Japan

98 major faults are selected for evaluation after the 1995 Kobe earthquake

Will be completed in 2004.

Sekiya fault, Tochigi pref.



Paleoearthquakes in Archeological Sites



写真5. 岩坪岡田島遺跡の砂脈（その2）.
Photo 5. Sand dykes in the Iwatsubo-Okadajima site (2).

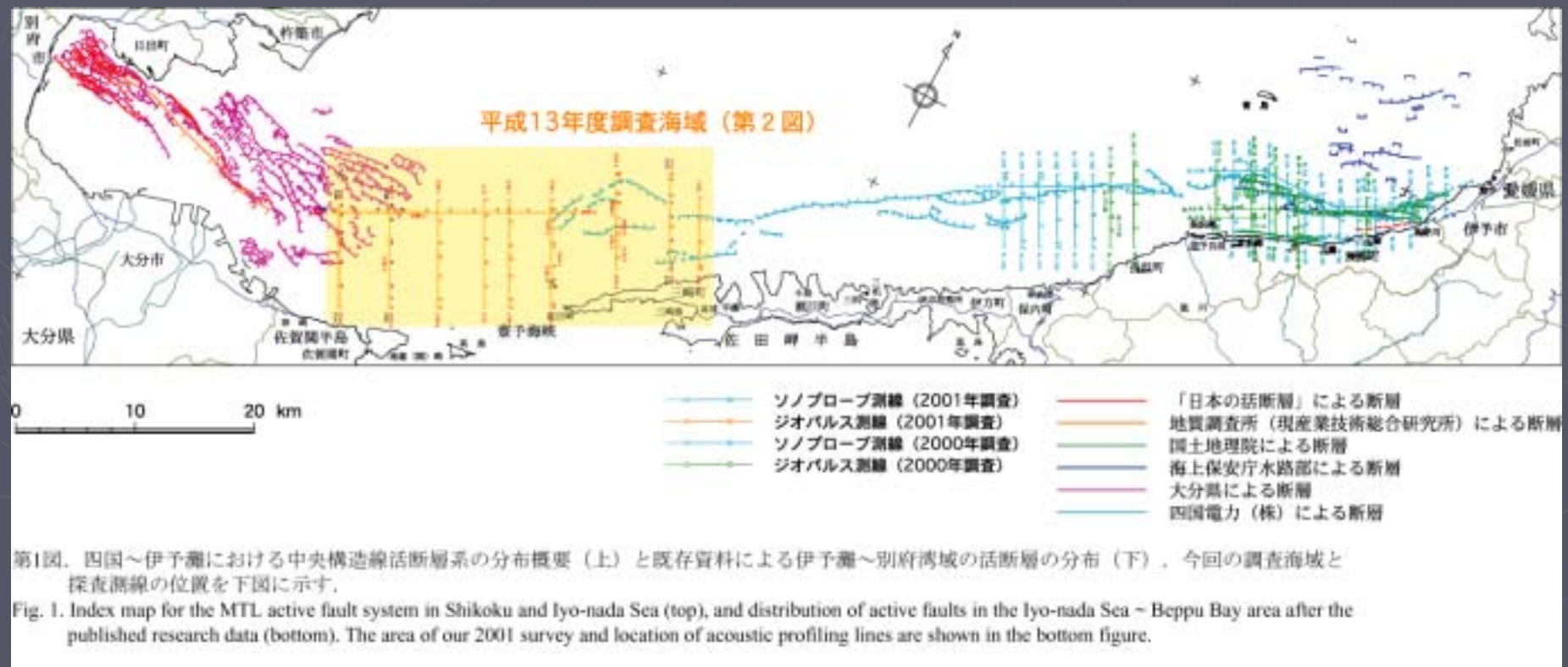


写真4. 岩坪岡田島遺跡の砂脈（その1）.
Photo 4. Sand dykes in the Iwatsubo-Okadajima site (1).

Submarine faults, Iyo-nada, MTL



Submarine faults, Iyo-nada, MTL

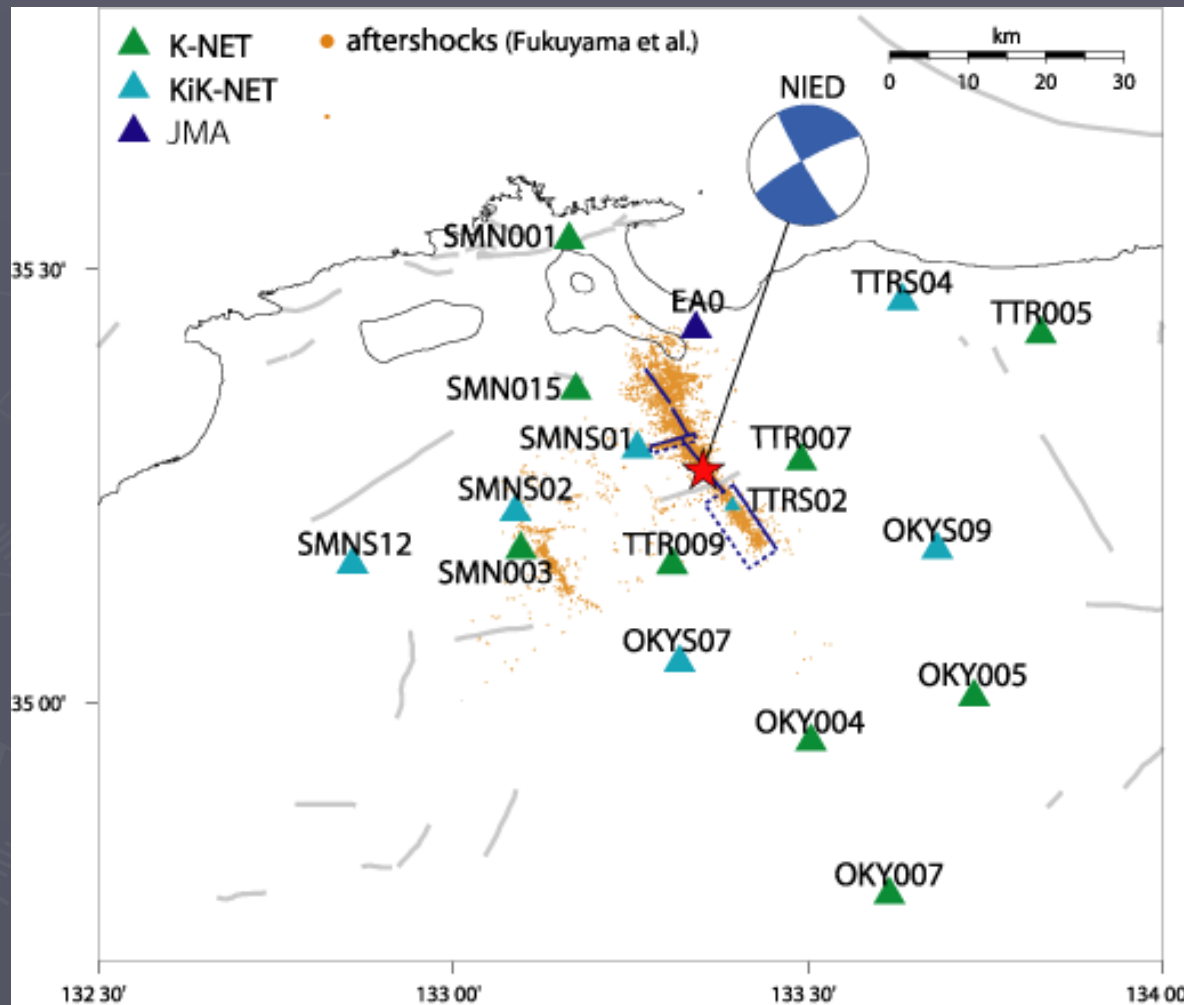


Geological cross-section of the Median Tectonic Line in Southwest Japan. The diagram shows a NW-SE profile. Key features include:

- Directional Labels:** NW (Northwest) and SE (Southeast).
- Faults:**
 - 下瀬沖北断層 (Lower Seto North Fault) indicated by a blue arrow on the left.
 - 瀬沖南断層 (Seto South Fault) indicated by a blue arrow on the right.
- Sampling Sites:**
 - Site 1:** Located in the center, with a core depth of 5.0m (標高差 5.0m).
 - Site 2:** Located on the right, with a core depth of 5.0m (標高差 5.0m).
- Soil Layers:** Various layers are labeled with letters and numbers, including:
 - a (海底面) - Seafloor
 - a1, a2
 - b
 - c (K-Ah)
 - d
 - e
 - f
 - g
 - h
 - i
 - j
 - k
 - l
 - m
 - n
 - o
 - p
 - q
 - r
 - s
 - t
 - u
 - v
 - w
 - x
 - y
 - z
 - aa
 - ab
 - ac
 - ad
 - ae
 - af
 - ag
 - ah
 - ai
 - aj
 - ak
 - al
 - am
 - an
 - ao
 - ap
 - aq
 - ar
 - as
 - at
 - au
 - av
 - aw
 - ax
 - ay
 - az
 - ba
 - bb
 - bc
 - bd
 - be
 - bf
 - bg
 - bh
 - bi
 - bj
 - bk
 - bl
 - bm
 - bn
 - bo
 - bp
 - bq
 - br
 - bs
 - bt
 - bu
 - bv
 - bw
 - bx
 - by
 - bz
 - ca
 - cb
 - cc
 - cd
 - ce
 - cf
 - cg
 - ch
 - ci
 - cj
 - ck
 - cl
 - cm
 - cn
 - co
 - cp
 - cq
 - cr
 - cs
 - ct
 - cu
 - cv
 - cw
 - cx
 - cy
 - cz
 - da
 - db
 - dc
 - dd
 - de
 - df
 - dg
 - dh
 - di
 - dj
 - dk
 - dl
 - dm
 - dn
 - do
 - dp
 - dq
 - dr
 - ds
 - dt
 - du
 - dv
 - dw
 - dx
 - dy
 - dz
 - ea
 - eb
 - ec
 - ed
 - ee
 - ef
 - eg
 - eh
 - ei
 - ej
 - ek
 - el
 - em
 - en
 - eo
 - ep
 - eq
 - er
 - es
 - et
 - eu
 - ev
 - ew
 - ex
 - ey
 - ez
 - fa
 - fb
 - fc
 - fd
 - fe
 - ff
 - fg
 - fh
 - fi
 - fj
 - fk
 - fl
 - fm
 - fn
 - fo
 - fp
 - fq
 - fr
 - fs
 - ft
 - fu
 - fv
 - fw
 - fx
 - fy
 - fz
 - ga
 - gb
 - gc
 - gd
 - ge
 - gf
 - gg
 - gh
 - gi
 - gj
 - gk
 - gl
 - gm
 - gn
 - go
 - gp
 - gq
 - gr
 - gs
 - gt
 - gu
 - gv
 - gw
 - gx
 - gy
 - gz
 - ha
 - hb
 - hc
 - hd
 - he
 - hf
 - hg
 - hh
 - hi
 - hj
 - hk
 - hl
 - hm
 - hn
 - ho
 - hp
 - hq
 - hr
 - hs
 - ht
 - hu
 - hv
 - hw
 - hx
 - hy
 - hz
 - ia
 - ib
 - ic
 - id
 - ie
 - if
 - ig
 - ih
 - ii
 - ij
 - ik
 - il
 - im
 - in
 - io
 - ip
 - iq
 - ir
 - is
 - it
 - iu
 - iv
 - iw
 - ix
 - iy
 - iz
 - ja
 - jb
 - jc
 - jd
 - je
 - jf
 - jj
 - jk
 - jl
 - jm
 - jn
 - jo
 - jp
 - jq
 - jr
 - js
 - jt
 - ju
 - jv
 - jw
 - jx
 - jy
 - jz
 - ka
 - kb
 - kc
 - kd
 - ke
 - kf
 - kg
 - kh
 - ki
 - kj
 - kl
 - km
 - kn
 - ko
 - kp
 - kq
 - kr
 - ks
 - kt
 - ku
 - kv
 - kw
 - kx
 - ky
 - kz
 - la
 - lb
 - lc
 - ld
 - le
 - lf
 - lg
 - lh
 - li
 - lj
 - lk
 - ll
 - lm
 - ln
 - lo
 - lp
 - lq
 - lr
 - ls
 - lt
 - lu
 - lv
 - lw
 - lx
 - ly
 - lz
 - ma
 - mb
 - mc
 - md
 - me
 - mf
 - mg
 - mh
 - mi
 - mj
 - mk
 - ml
 - mm
 - mn
 - mo
 - mp
 - mq
 - mr
 - ms
 - mt
 - mu
 - mv
 - mw
 - mx
 - my
 - mz
 - na
 - nb
 - nc
 - nd
 - ne
 - nf
 - ng
 - nh
 - ni
 - nj
 - nk
 - nl
 - nm
 - nn
 - no
 - np
 - nq
 - nr
 - ns
 - nt
 - nu
 - nv
 - nw
 - nx
 - ny
 - nz
 - oa
 - ob
 - oc
 - od
 - oe
 - of
 - og
 - oh
 - oi
 - oj
 - ok
 - ol
 - om
 - on
 - oo
 - op
 - oq
 - or
 - os
 - ot
 - ou
 - ov
 - ow
 - ox
 - oy
 - oz
 - pa
 - pb
 - pc
 - pd
 - pe
 - pf
 - pg
 - ph
 - pi
 - pj
 - pk
 - pl
 - pm
 - pn
 - po
 - pp
 - pq
 - pr
 - ps
 - pt
 - pu
 - pv
 - pw
 - px
 - py
 - pz
 - qa
 - qb
 - qc
 - qd
 - qe
 - qf
 - qg
 - qh
 - qi
 - qj
 - qk
 - ql
 - qm
 - qn
 - qo
 - qp
 - qq
 - qr
 - qs
 - qt
 - qu
 - qv
 - qw
 - qx
 - qy
 - qz
 - ra
 - rb
 - rc
 - rd
 - re
 - rf
 - rg
 - rh
 - ri
 - rj
 - rk
 - rl
 - rm
 - rn
 - ro
 - rp
 - rq
 - rr
 - rs
 - rt
 - ru
 - rv
 - rw
 - rx
 - ry
 - rz
 - sa
 - sb
 - sc
 - sd
 - se
 - sf
 - sg
 - sh
 - si
 - sj
 - sk
 - sl
 - sm
 - sn
 - so
 - sp
 - sq
 - sr
 - ss
 - st
 - su
 - sv
 - sw
 - sx
 - sy
 - sz
 - ta
 - tb
 - tc
 - td
 - te
 - tf
 - tg
 - th
 - ti
 - tj
 - tk
 - tl
 - tm
 - tn
 - to
 - tp
 - tq
 - tr
 - ts
 - tt
 - tu
 - tv
 - tw
 - tx
 - ty
 - tz

Fig. 2. Sedimentary columns of the Site 1 and Site 2 cores projected on the high-resolution acoustic profile of No. 51 line.

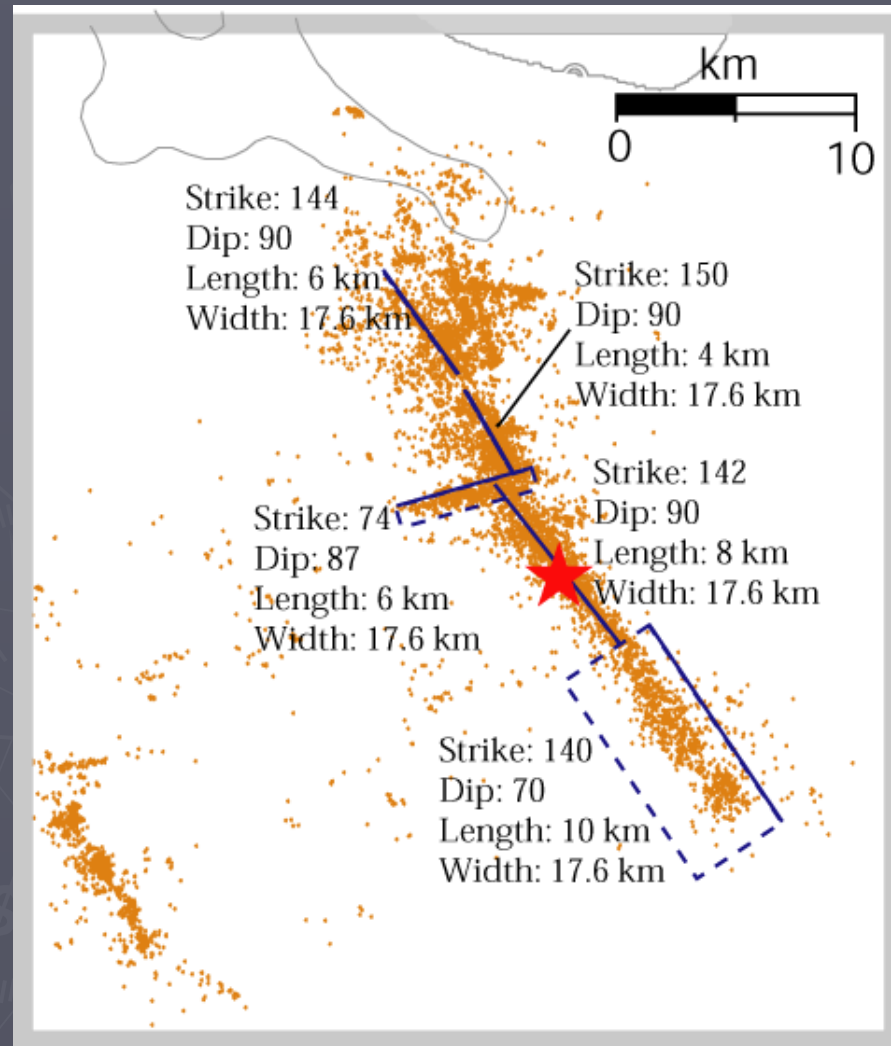
Tottori-ken Seibu earthquake of Nov. 6, 2000 (M7.3_{JMA})



第1図. 観測点および仮定した断層の位置. ▲が観測点を示し、太い実線が断層を示す。

Fig. 1. Map showing strong motion stations used in this study (triangle) and fault locations.

Fault Model of the 2000 Tottori-ken Seibu earthquake

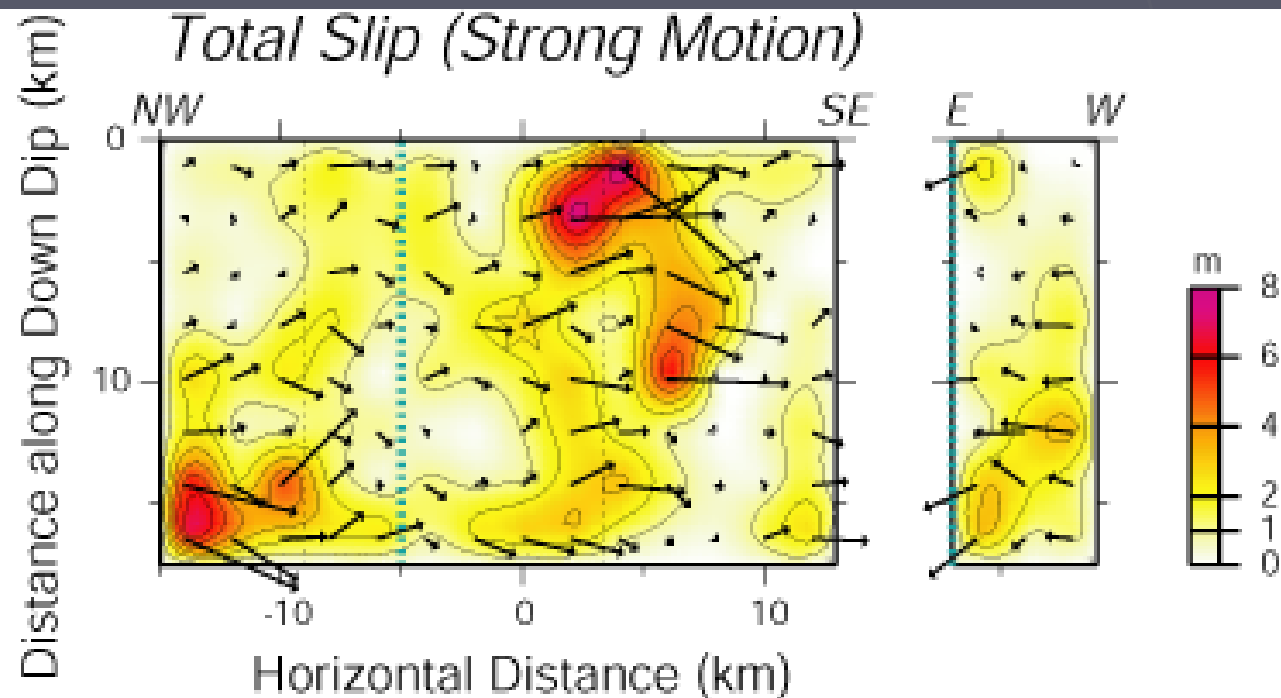


第2図. 強震動記録を解析する際に仮定した断層モデル.
Fig. 2. Fault model used in analysis of strong ground motion data.

We expected surface ruptures >10km. but....

From Horikawa et al, (2001)

Distribution of total slip on faults

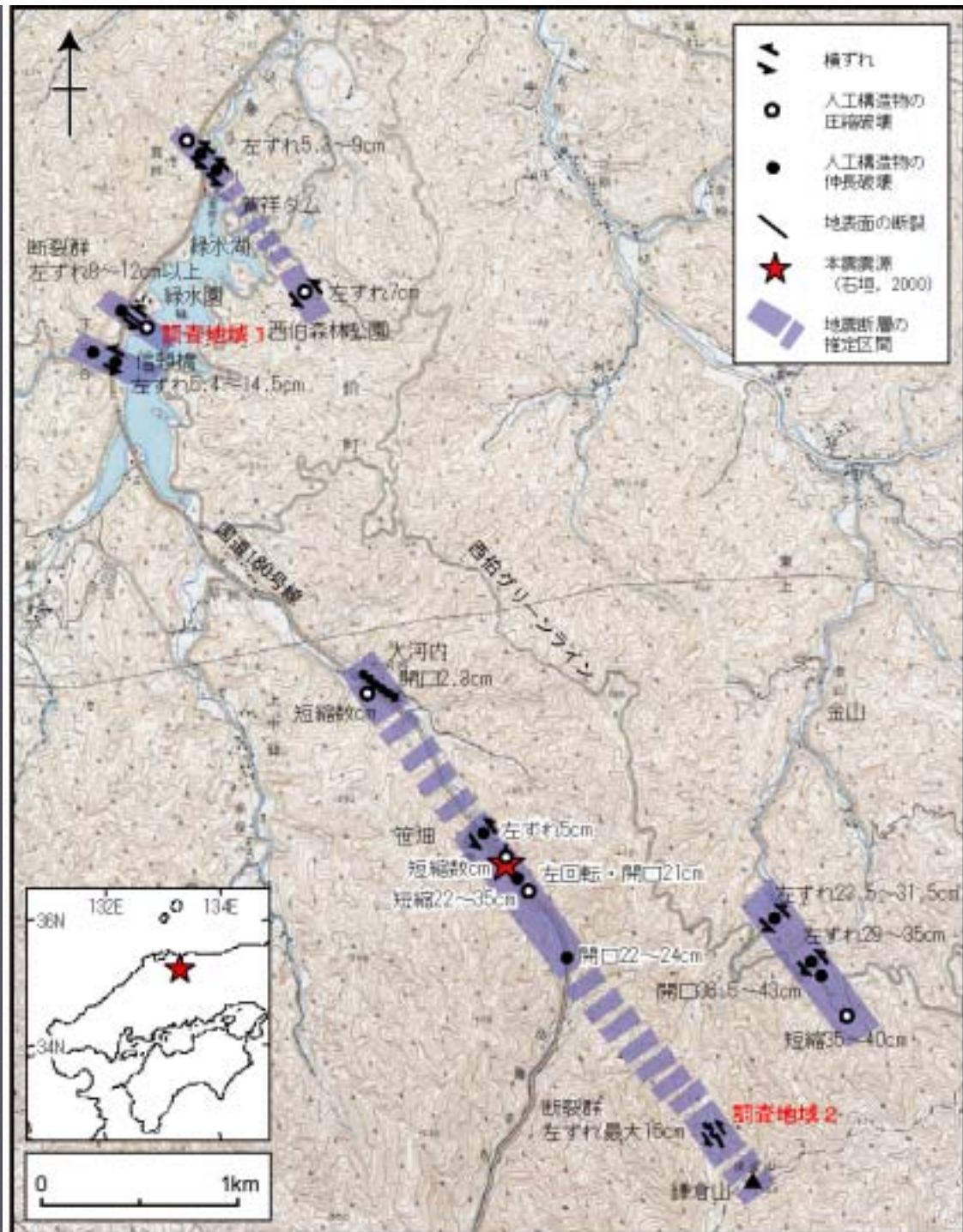


From Horikawa et al, (2001)

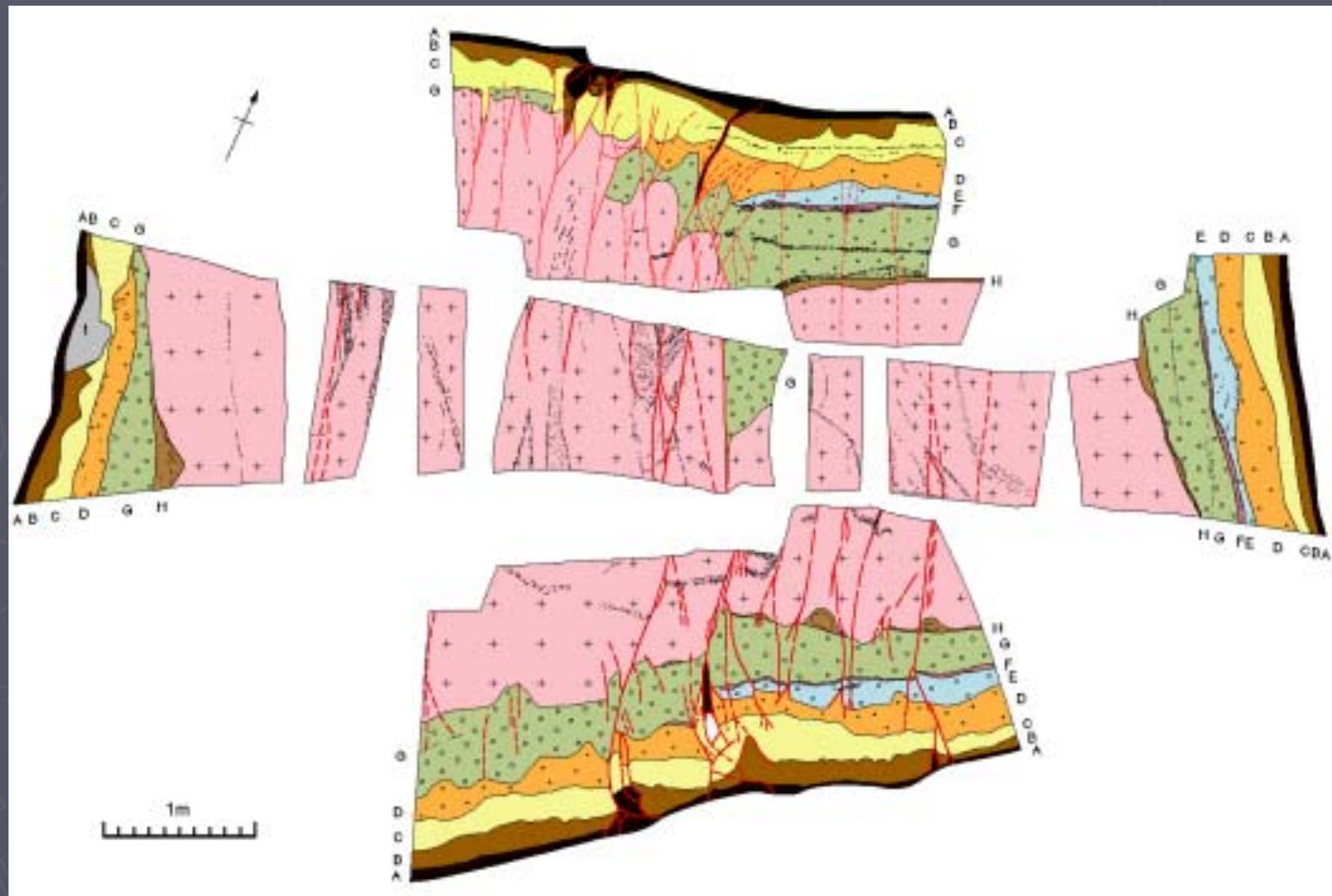
第3図. 最終すべり量（全てのtime windowからの寄与の総和）の断層面上での分布。
星印は破壊開始点を示す。左側の断層は北西-南東走向の断層群、右側の断層はN74° E走向の断層。それぞれの断層に示した緑色の線が分岐位置を示す。断層の配置は第2図を参照。
Fig. 3. Distribution of total slip on faults. The total slip is a sum of contribution from all time windows. A star means the hypocenter. Left: faults striking NW-SE, right: a fault striking N74°E. Green dotted lines show the location at which the two fault systems intersect. See also Fig. 2 for the fault configuration.

Surface ruptures and Trench sites

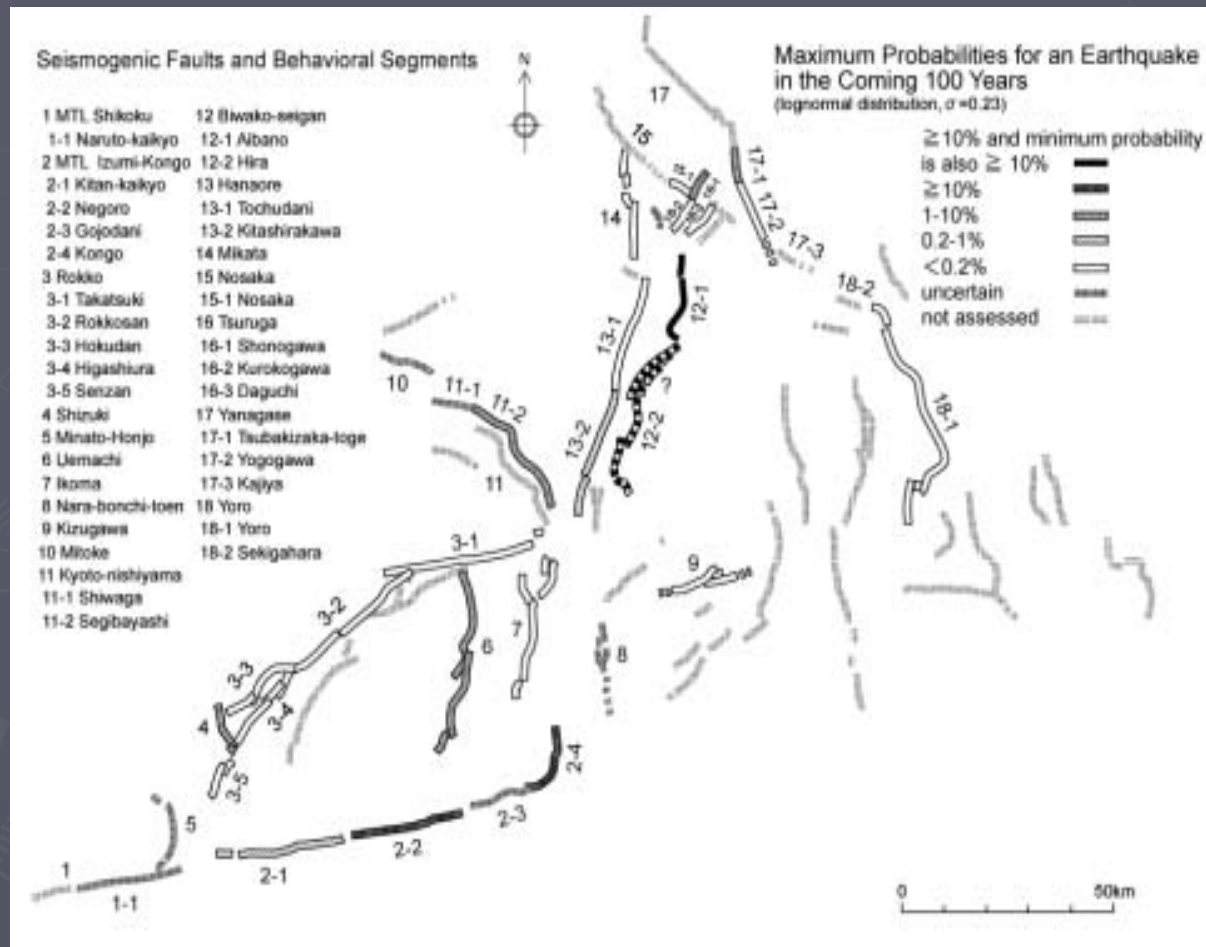
Modified from
Fusejima, Y.
et al (2001)



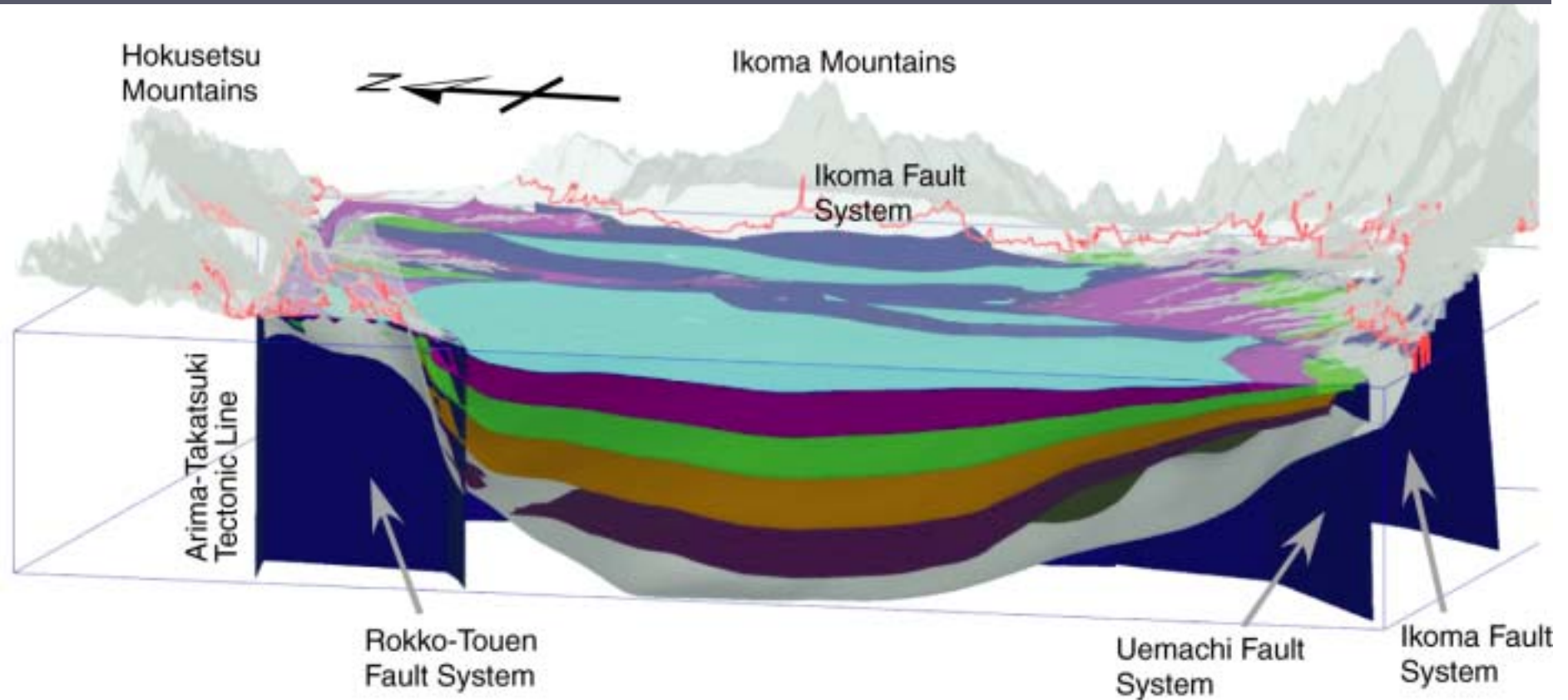
Trench log at the Kamakura-yama site






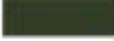



Fault Activity Evaluation



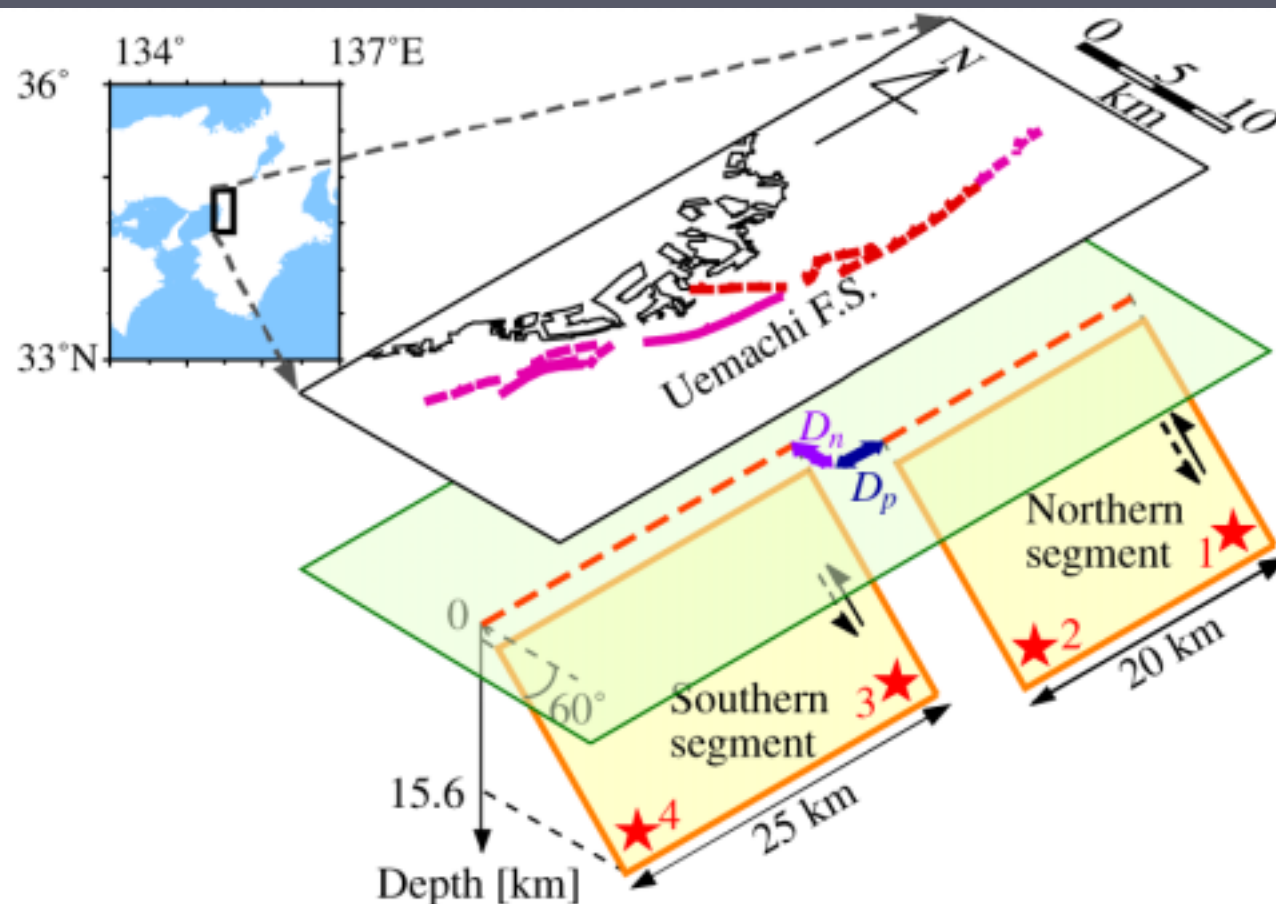
3D geological structure model of Osaka basin



第7図. 3次元地質構造モデルの可視化例。大阪湾側から東を見たもの。
Fig. 7. An example of visualization of the three-dimensional geologic structure model. East view from Osaka Bay.

Legends			
	Top of Ma 10		Gauss/Matuyama boundary
	Bottom of Ma 3		Top of Miocene series
	Bottom of Ma -1		Top of basement
	Fukuda tephra		

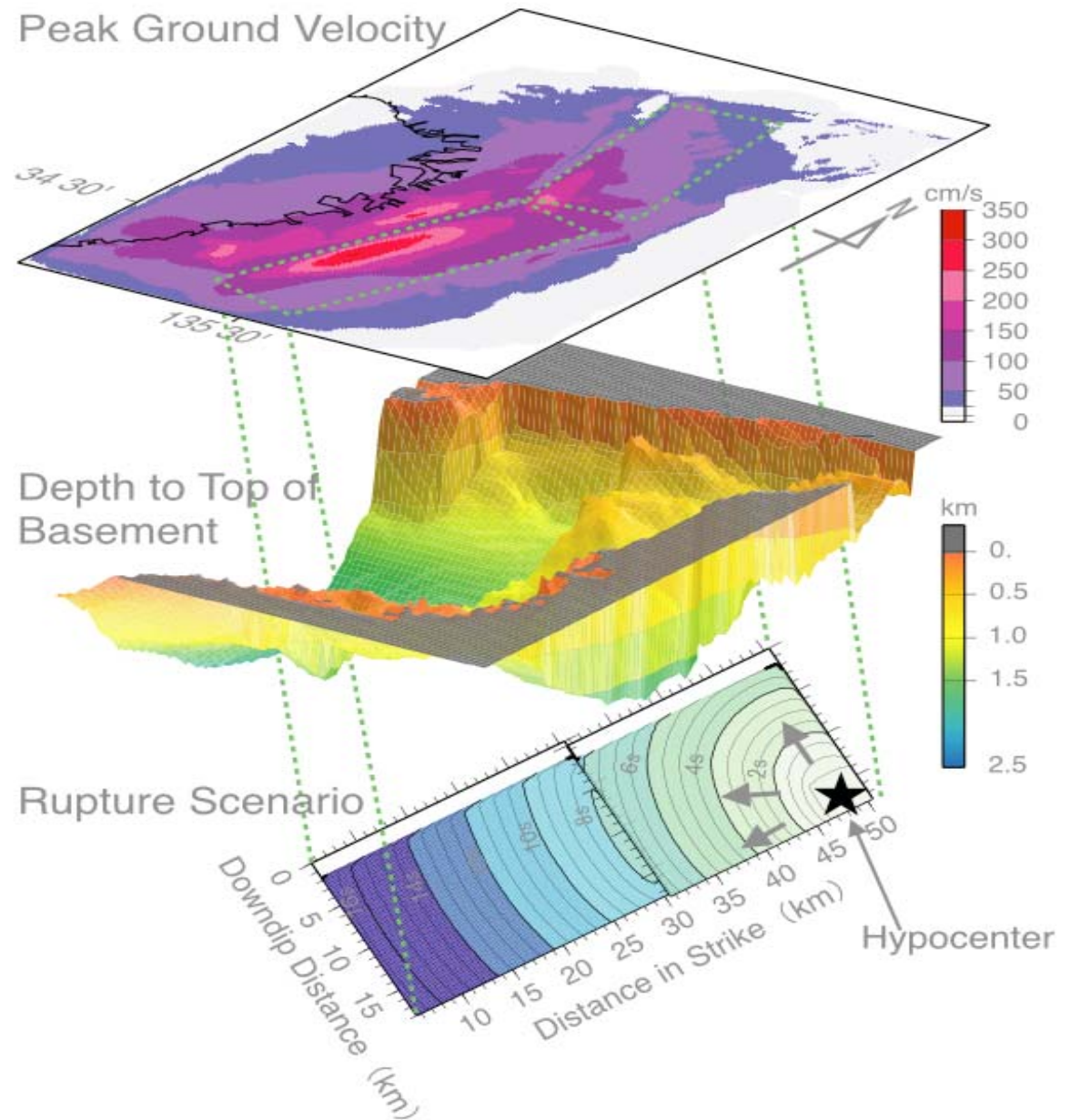
Fault model of Uemachi fault, Osaka pref.



第1図. 断層モデル. 地図 (水野ほか, 2002 による) 上のピンク色実線, ピンク色点線, 赤線は, それぞれ, 活断層 (主として後期更新世以降に活動したもの), 推定活断層, 沖積面下に伏在する活断層を示す. D_p と D_n は, それぞれ, 断層に平行な方向, 直交する方向の距離を示す. 星印は破壊開始点の位置の候補を示す.

Fig. 1. Fault model used in this study. In a map after Mizuno et al. (2002), pink solid and dotted lines indicate active faults (mainly active in the Late Pleistocene and Holocene) and inferred active faults, respectively. Red lines indicate active faults concealed beneath the alluvial plain. D_p and D_n indicate fault-parallel and fault-normal distances, respectively. Red stars are candidate locations for an initial crack.

Strong Motion Evaluation in Osaka Basin



International cooperation in AFRC, GSJ-AIST

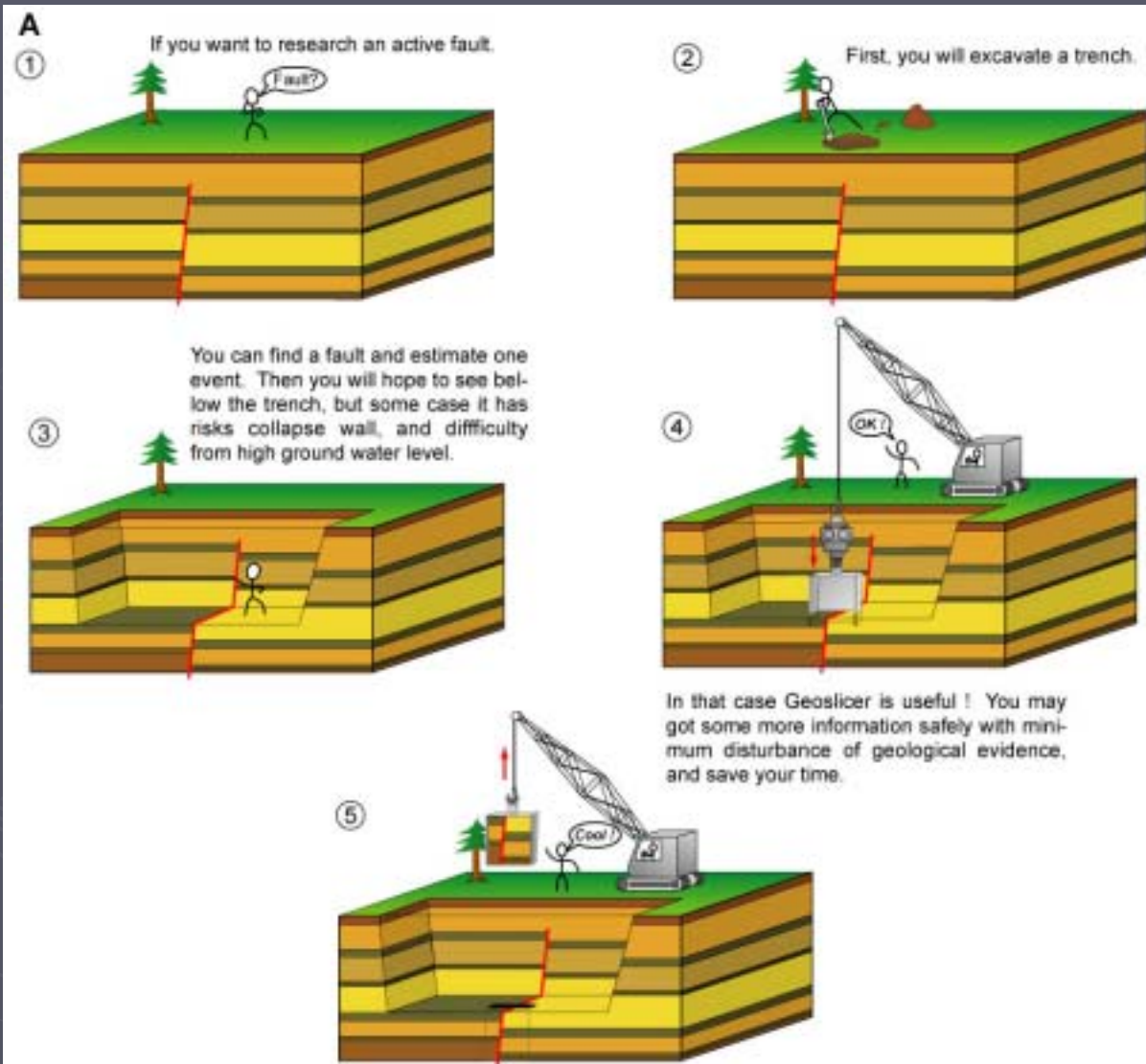
Introduction of Geo-slicers to USA,
Columbia river, Arkansas, Hayward fault
Tsunamis, USA, Chile

1999 Izmit and Duzce earthquakes, Turkey

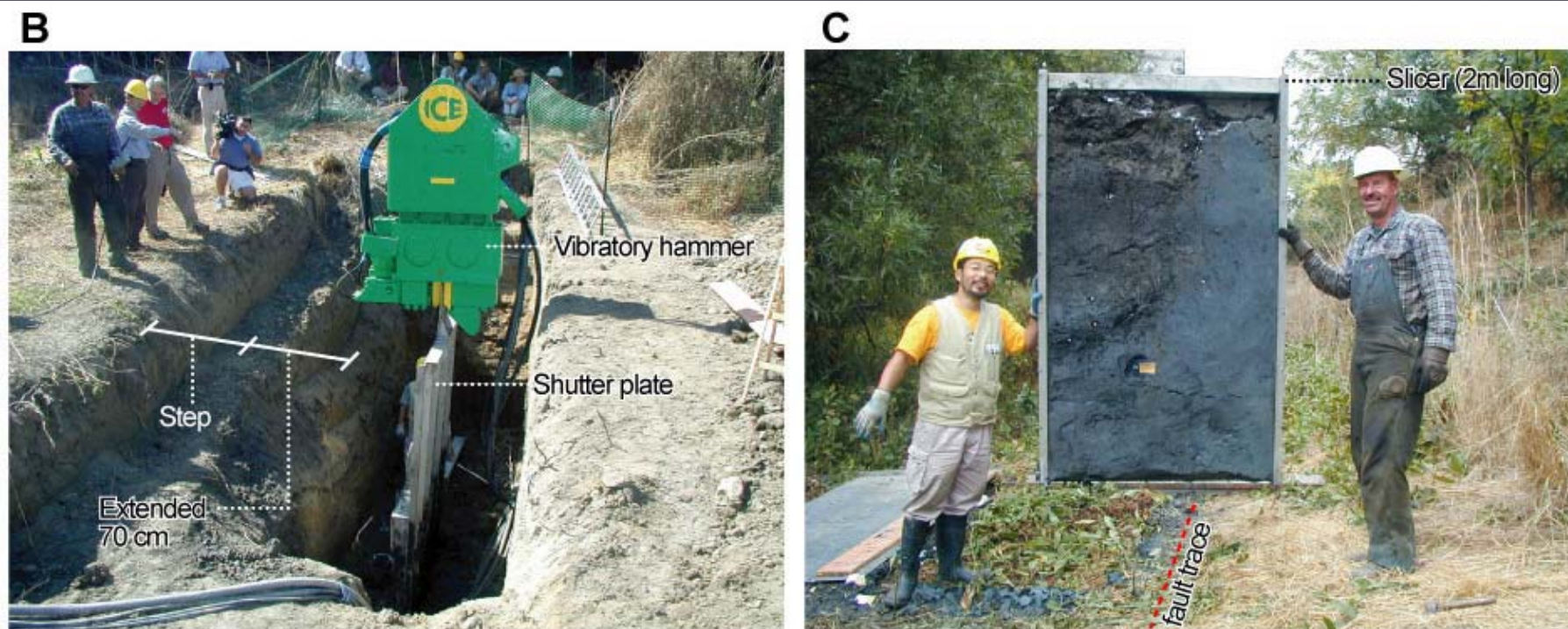
1999 Chi-chi Taiwan earthquake

2001 Kunlun-shan eq. China

Deeper geology below trenches



Hayward fault



第2図. 活断層トレンチ調査へのジオスライサーの適用. A: 調査のながれ, B: シャッタープレートの打ち込み, C: 抜き取られた試料断面 (GS-2) .

Fig. 2. Application of geoslicer to active fault research at conventional trench sites. A: flow of the survey, B: driving a geoslicer from the bottom of the trench, C: an extracted geoslice showing layers displaced by faults.

New evidence for earthquake over 2000 years, Washington State

Geoslicers
Liquefactions
Columbia river

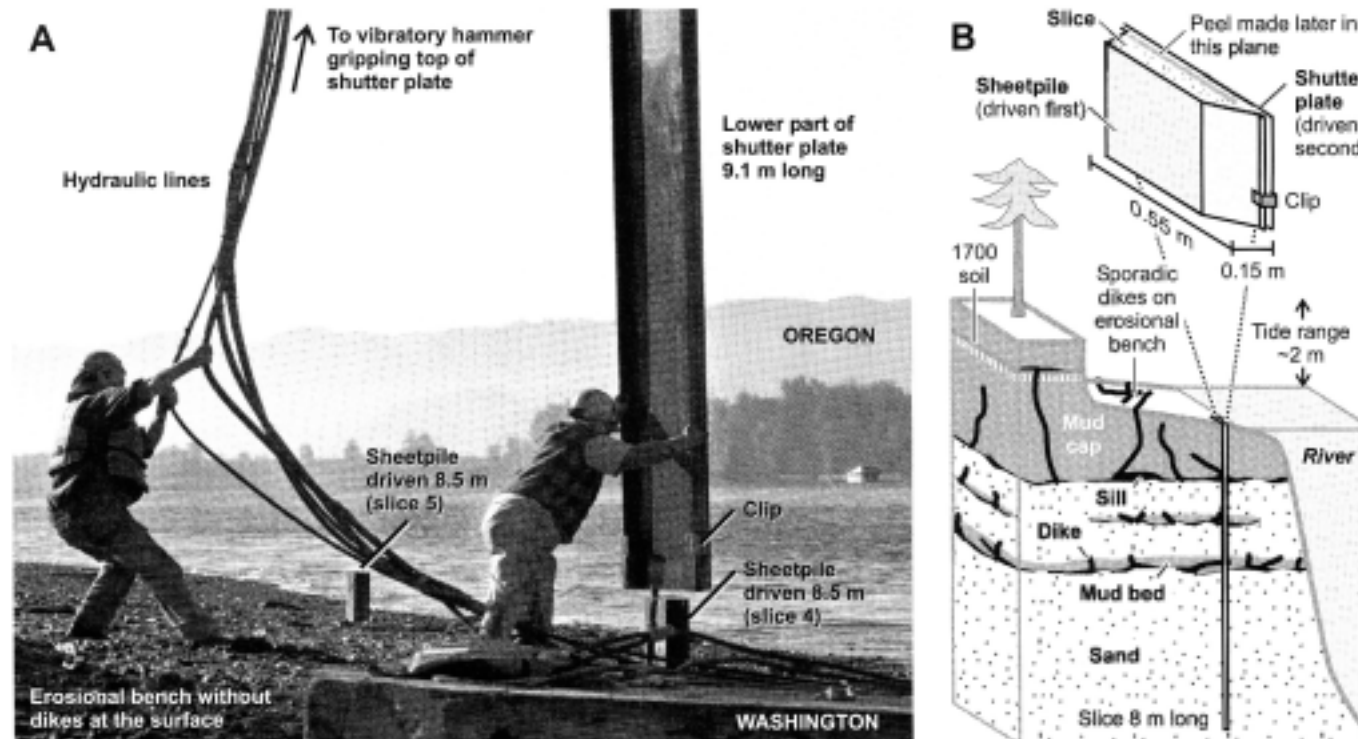


Fig. 1. (a) In this photo, geoslicing is in progress along the Columbia River at Hunting Island, Washington. (b) The diagram gives a schematic view of a slice in the area shown in (a). Photograph courtesy of Bill Wagner, Longview Daily News, September 26, 2000.

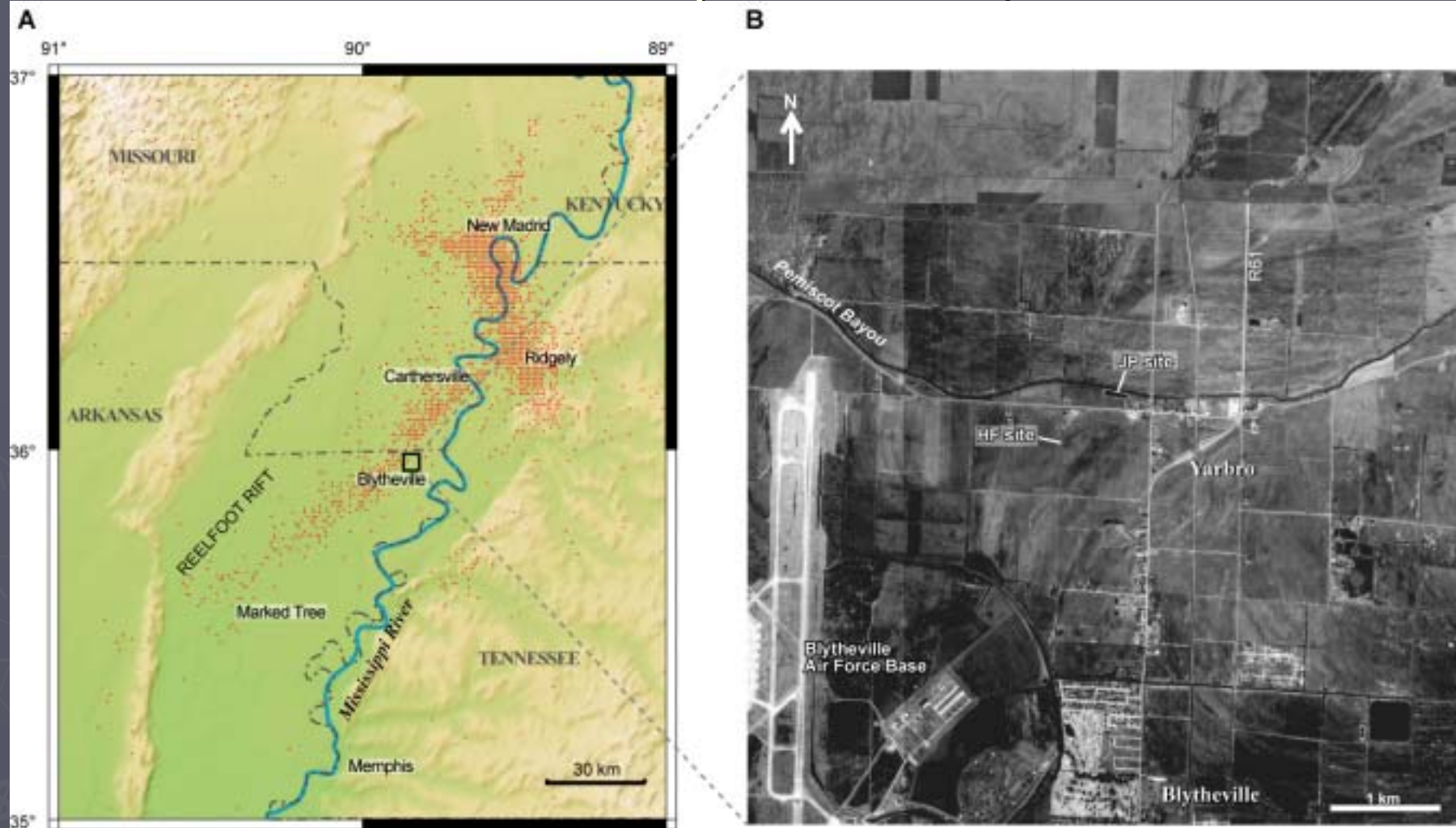


Fig. 2. Hunting Island adjoins the inferred rupture area of the 1700 Cascadia earthquake.

Brian F. Atwater et al.

Eos, Vol. 82, No.49, Dec. 4, 2001, p 603-608

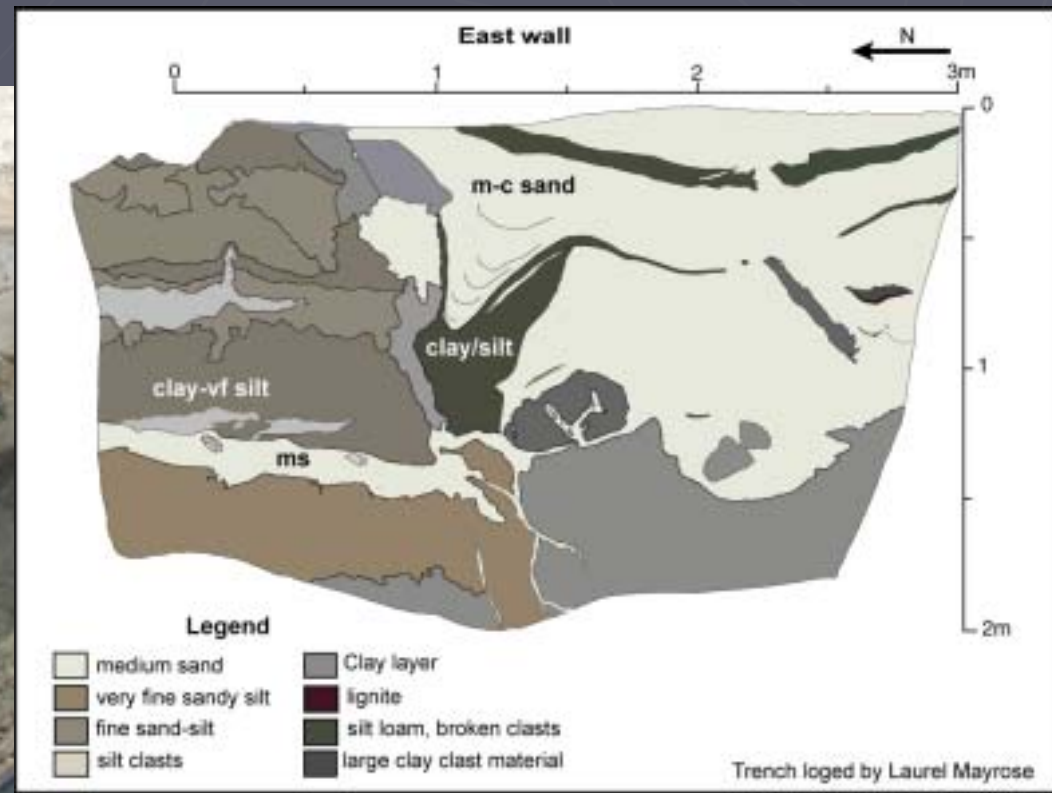
New Madrid Earthquake Zone, Arkansas



第1図. ニューマドリッド地震帯における最近の地震活動 (A) と調査地点周辺の空中写真 (B). 震央分布 (1974-2000) はCenter for Earthquake Research and Information (CERI) による。空中写真は、U.S. Geological Survey: 10 Apr. 1996 および16 Feb. 1994を使用。

Fig. 1. Index map of survey site. A: seismicity of New Madrid seismic zone, B: aerial photographs around the study site. The epicenter data (1974-2000) are from Center for Earthquake Research and Information (CERI) and the aerial photographs were taken by U.S. Geological Survey on 10 April 1996 and 16 February 1994.

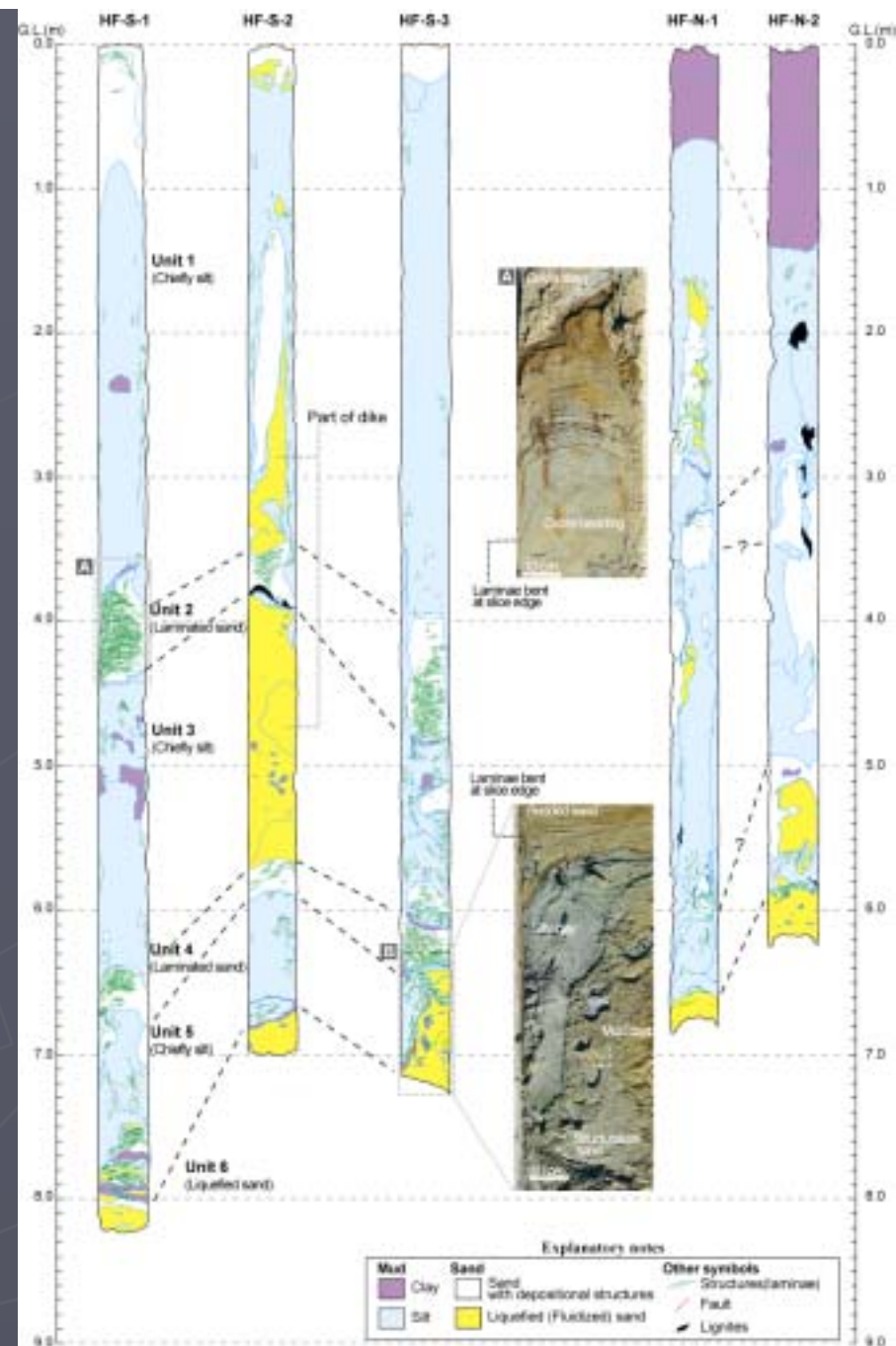
New Madrid Earthquake Zone, Arkansas



第4図. JPサイトトレンチで観察された噴砂構造.
Fig. 4. Sand blow feature on the trench wall at the JP site.

The geoslicing at two sites near Blytheville, Arkansas

In the fall of 2001, a US-Japan team made geoslicer surveys of liquefaction features in the New Madrid seismic zone of the central United States in hopes of improving methods for estimating ground motions from historic and prehistoric earthquakes. Large earthquakes occurred on December 16 (twice), 1811, and on January 23 and February 7, 1812 at the New Madrid seismic zone. Ground shaking from these earthquakes, which were felt as far away as on the Atlantic coast and Gulf of Mexico, produced thousands of sand blows on floodplains of the Mississippi River and nearby streams in an area at least 80 km by 200 km. Prehistoric sand blows, recognized in part by stratigraphic relations with Native American horizons and features, show that earthquake sequences produced similar liquefaction fields in this area about A. D. 800-1000 and 1300-1600.



第6図. HFサイトの試料スケッチ。写真A, Bの位置はスケッチ中に示す。
Fig. 6. Logs and photos (A and B) of geoslices at the HF site.

The geoslicing at two sites near Blytheville, Arkansas

The geoslicing was done at two sites near Blytheville, Arkansas (sites JP and HF). A trench at the JP site, excavated by USGS and the University of Memphis, showed a sand blow of fine to medium sand with many mud clasts. On the ditch wall at the HF site, a sand blow intrudes a paleosol containing artifacts about 1 m below the surface, and almost reaches the ground surface.

Using long and wide slicers, we extracted soil sections including liquefaction features. The stratigraphy in the slices at each site shows that the sand blows came from depths of 7 m or more. A sand blow on the ditch wall (HF site) continues to a dike observed in the slice 4 m beneath.

Detrital wood in the highest potential source sand beneath the JP site gave radiocarbon ages corresponding to A.D. 970-1190 and A.D. 1000-1170. These ages show that the sand was shaken not only in 1811-1812 but perhaps also during the earthquake sequence of A.D. 800-1000.